CTCCTCTTCAC(C/T)ATGATATTTGT; α2, α4 CTCTTCACCATGAT(A/C)TTTG; α7: ATGCCAGCAACATCTGATTCT and β TGGT(A/G)CTGGTGACCTTCTC. Antisense primers: (reverse complement of sequences specified by number) α2: 1367 to 1386; α3: 1305 to 1325; α4: 1201 to 1221; α5: 1164 to 1184; α7: TACTACAGAGGCTGCAAACTT and β: ACCATGGC(A/C)AC(A/G)TACTT.

7. We ran 2.5 μg of poly(A)$^+$ RNA from ED10 sympathetic ganglia per lane on a formaldehyde (1%) agarose gel and blotted it onto Nytran (Schleicher and Schuell) for hybridization, according to the manufacturer's instructions. Probes generated by random primer synthesis (Promega) to a specific activity of ≥5 × 10^8 cpm/μg. Following the lack of hybridization to α2 probe, the lane was rehybridized to other probes to confirm RNA retention on the blot.
8. I. Silman and A. Karlin, *Science* **164**, 1420 (1969).
9. R. Gardette *et al.*, *Dev. Biol.* **147**, 83 (1991).
10. Methods: E10 and 11 chick lumbar sympathetic ganglion neurons were prepared as described (*4*) and plated in dishes with a 13-mm sunken well of ~150 μl. BAC bromide treatment was modified from P. Leprince [*Biochemistry* **22**, 5551 (1983) (*9*)]. Oligonucleotide treatment: Functional block oligonucleotides: α3 sense and antisense −77 to −63; α3 mismatch antisense CGACCGTAAAACAAC; α4 antisense −69 to −55; α7 antisense GCATCAGCGCCCGGA. Oligos made on Applied Biosystems Automated DNA Synthesizer (380B) and purified by polyacrylamide gel electrophoresis and reversed-phase chromatography (*5*). No known chick AChR sequences are complementary to these 15-mers (optimal complementarity with other AChR sequences ≤72%). Oligonucleotides in growth media (*4*) were added to neurons within culture wells and maintained in a humidified chamber (48 hours). Additional antisense controls: neither inclusion of α3 antisense in the recording pipette nor treatment of neurons with oligonucleotides similar to α3 in size, charge, or sequence (three base mismatch) had any effect on AChR function. K$^+$-channel activity and GABA-evoked currents were unaltered in antisense-treated neurons.
11. Single channel and macroscopic current analysis. Data acquisition and analysis used BASIC 23–based software developed by S. Schuetze (*4*) or S. Siegelbaum. Slope conductance determined from recordings at −30, −50, and −70 mV relative to rest. We obtained mean single channel current activity in individual patches by integrating t(open)/t(total) for the first 3 min (cell-attached patch) or for 10 s after agonist application (outside-out). The decay time course of macroscopic currents was fit by the sum of two exponential functions (fast and slow time constants τ_1 and τ_2). Presentation and statistics. Mean single channel current and macroscopic current decay time constant data were not normally distributed and therefore are presented in box plots. The central box shows the middle 50% of the data (25th through 75th percentiles); the horizontal line indicates the median, and the whiskers indicate the range of data values (10th through 90th percentiles). Outliers, if present, are plotted as asterisks. Mean current and decay constants of control groups were normalized to permit statistical comparison between corresponding experimental groups. The values obtained were normally distributed following log transformation [Kolmogorov-Smirnov test; G. W. Snedecor and W. G. Cochran, *Statistical Methods* (Iowa State Univ. Press, Ames, IA, ed. 6, 1967), p. 329; NPAR and MGLH modules of Systat™]. Subsequent analysis of variance (ANOVA) was followed by a test for multiple comparisons between pairs of group means based on unequal sample sizes.
12. AChR number in α3 antisense–treated neurons: ACh dose response data indicate that 500 μM evokes a maximal response in both control and α3 antisense–treated neurons. Mathematical subtraction of the contribution of slower desensitization indicates that α3 antisense decreased the number of activatable AChRs by >65% (rather than 58%). This correction is still an underestimate because it assumes comparable single-channel conductances in α3 antisense–treated and control neurons whereas larger conductance channels predominate in α3 antisense–treated neurons. (L versus α3 AS-L: 66% versus 89% of patches; XL versus α3 AS-Giant: 37% versus 52% of patches).
13. S. Couturier *et al.*, *J. Biol. Chem.* **265**, 17560 (1990).
14. S. Couturier *et al.*, *Neuron* **5**, 847 (1990).
15. The residual current in neurons treated with α3 antisense plus α7 antisense or α-BGT resembles control in desensitization kinetics and in its complete block by nBGT [R. Loring and R. Zigmond, *Trends Neurosci.* **11**, 73 (1988)]. This current may be composed of native receptors assembled from the internal pool or due to delayed or incomplete antisense-mediated deletion.
16. R. T. Boyd *et al.*, *Neuron* **1**, 495 (1988); R. Schoepfer *et al.*, *FEBS Lett.* **257**, 393 (1989).
17. P. Blount and J. P. Merlie, *Neuron* **3**, 349 (1989).
18. R. L. Huganir and P. Greengard, *ibid.* **5**, 555 (1990).
19. A. Brussaard, J. Doyle, L. Role, in preparation.
20. We thank R. Axel, T. Jessell, A. Karlin, and S. Siegelbaum (Columbia College of Physicians and Surgeons) for discussions, reagents, and extensive comments on the manuscript; M. Ballivet and collaborators from the University of Geneva for sharing clones and sequence information before publication; and D. King, A. Roy, A. Dolorico, A. Witty, and E. Hubel for technical assistance. Supported by awards from NSF, North Atlantic Treaty Organization, Muscular Dystrophy Association, NIH (NS27680, NS 29071), and the Council for Tobacco Research.

12 June 1991; accepted 10 October 1991

Refined Structure of Charybdotoxin: Common Motifs in Scorpion Toxins and Insect Defensins

FRANCOIS BONTEMS, CHRISTIAN ROUMESTAND, BERNARD GILQUIN, ANDRÉ MÉNEZ, FLAVIO TOMA

Conflicting three-dimensional structures of charybdotoxin (Chtx), a blocker of K$^+$ channels, have been previously reported. A high-resolution model depicting the tertiary structure of Chtx has been obtained by DIANA and X-PLOR calculations from new proton nuclear magnetic resonance (NMR) data. The protein possesses a small triple-stranded antiparallel β sheet linked to a short helix by two disulfides and to an extended fragment by one disulfide, respectively. This motif also exists in all known structures of scorpion toxins, irrespective of their size, sequence, and function. Strikingly, antibacterial insect defensins also adopt this folding pattern.

CHARYBDOTOXIN (CHTX) IS A TOXIN acting on K$^+$ channels isolated from venom of a scorpion (*Leiurus quinquestriatus hebraeus*) (*1*). It is a small protein, containing 37 amino acids and three disulfide bridges (*2*). Elucidation of its three-dimensional (3-D) structure is important for understanding the molecular basis of its activity and for designing drugs acting on K$^+$ channels. The structure of Chtx has been reported in two recent NMR studies (*3, 4*) that led to different 3-D models of the toxin. One of these has now been retracted (*5*). Also, a recent communication has reported the preliminary NMR structure of synthetic Chtx (*6*) that is similar to that obtained in our work. We have collected additional NMR data from which further Chtx structures have been computed. The new refined structures confirm our initial model (*4*) and show that Chtx possesses a motif that is conserved in functionally unrelated proteins of arthropods.

We have reported elsewhere the sequence-specific assignments of the ^{1}H NMR spectra, the identification of the secondary structure elements, and the tertiary structure computations (*4*). The new data, recorded at temperatures from 15° to 45°C, include NOEs (eight mixing times from 50 to 300 ms), HN-Hα and Hα-Hβ vicinal coupling constants, and amide ^{1}H-^{2}H exchange rates at 15°C. Iteration of back calculations and analysis of NOESY experiments led to the assignment of 144 interresidue NOE connectivities that correspond to 72 sequential and 72 nonsequential effects (Fig. 1). Intensities of backbone-backbone NOEs were determined either from NOE buildup rates or from cross-peak volumes in spectra recorded with a 150-ms mixing time. The corresponding distance constraints were obtained calibrating the backbone-backbone NOE intensities with known distances in regular secondary structures (2.2 Å for $d_{\alpha N}$ in a β sheet and 2.8 Å for d_{NN} in an α helix). Measurement of the exchange rates of amide protons allowed the identification of 11 hydrogen bonds, leading to the introduction of 22 additional constraints. In addition, 12 χ1-angle values, including those of the six half-cystines, were deduced from the measurement of $^3J_{H\alpha\text{-}H\beta}$ and the identification of intraresidue HαHβ NOEs, whereas 30 φ-angle values were deduced from the values of $^3J_{HN\text{-}H\alpha}$ coupling constants.

The 3D-structures of Chtx were derived from these data with a procedure that combined minimization in the dihedral angle

Département d'Ingénierie et d'Etudes des Protéines, CEN Saclay, 91191 Gif sur Yvette, France.

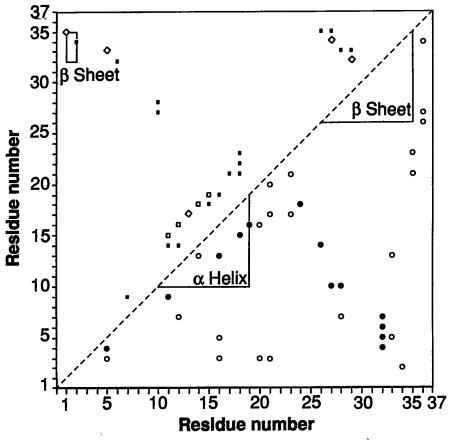

Fig. 1. Diagonal plot of NOEs used for the computations of Chtx structures. Each off-diagonal point indicates one effect (or more) between residues at positions shown along the axis. Above the diagonal: (■) backbone-backbone NOEs; (□) hydrogen bonds; and (◇) NOEs and hydrogen bonds. Below the diagonal: (●) Backbone–side chain NOEs and (○) side chain–side chain NOEs.

Fig. 2. Three-dimensional structures of Chtx (*21*). (**Top**) Superimposition of eight structures of Chtx with two different orientations. Disulfides have been omitted for a more clear presentation. (**Bottom**) Presentation of one structure of Chtx with the three disulfides (dashed lines). Glp is py Glu (Z).

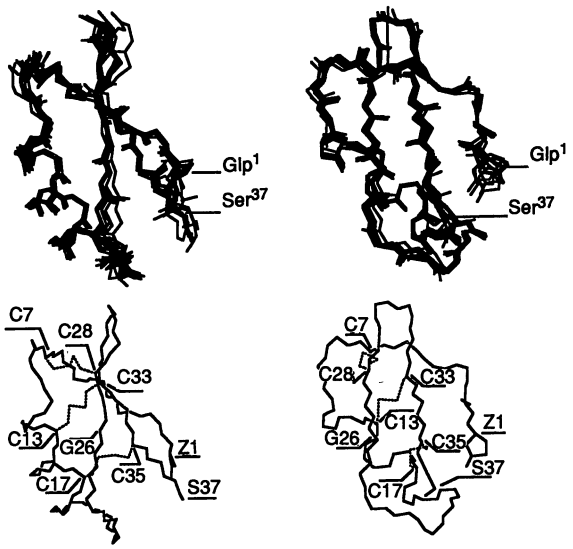

space [program DIANA (*7*)] and refinement by simulated annealing [program X-PLOR (*8*)]. A set of 25 structures was first computed with DIANA. The 12 best structures [1.2 Å root-mean-square (rms) deviation, no distance violation greater than 1.0 Å] were further refined with X-PLOR. The simulated annealing protocol consisted mainly in 10,000 steps of dynamics at 1000 K followed by 40,000 steps of slow cooling to 0 K. All of the final structures have a total energy less than -2500 kJ mol^{-1} and present no distance violation greater than 0.1 Å. The average rms deviation for the 12 structures is 0.68 Å. As shown in Fig. 2, Chtx has a globular structure consisting of a small triple-stranded β sheet (sequences 1 to 2, 25 to 29, and 32 to 36) linked respectively, to a well-defined α helix (sequence 11 to 19) by two disulfides (sequences 13 to 33, and 17 to 35) and to an extended fragment (sequence 4 to 7) by the third disulfide (sequence 7 to 28). The axis of the sheet forms a 45° angle with the axis of the helix and a 90° angle with the direction of the 4 to 7 extended fragment. The helix is connected to both the 4 to 7 extended fragment and the 25 to 29 β strand by two loops; the two β strands 25 to 29 and 32 to 36 are connected by a well-defined type I β turn. The structure of Chtx seems to be stabilized by both the three disulfides and a hydrophobic cluster comprising the side chains of Thr[3], Val[5], Val[16], and Leu[20].

Charybdotoxin and related toxins that act on K^+ channels are minor components of scorpion venoms. The other scorpion toxins are markedly different in several aspects. Most of them recognize Na^+ channels in insects or mammals instead of K^+ channels. Their polypeptide chain (60 to 65 residues) is nearly twice as long as that of Chtx and has four disulfides. Their primary structures share little similarities with that of Chtx (*9*). Strikingly, however, inspection of all known secondary or tertiary structures of scorpion toxins, obtained by either NMR (*10–13*) or x-ray crystallography (*14, 15*), revealed to us that all of them possess a triple-stranded β sheet, an α helix, an extended fragment, and three disulfides. These structural elements are organized as in Chtx. In order to better characterize these similarities, we proceeded to a quantitative comparison of the structure of Chtx with those of two long-chain toxins, the variant 3 from *Centruroides sculpturatus Ewing* (*14*) and the toxin II from *Androctonus australis Hector* (*15*), whose atomic coordinates were available. As shown in Fig. 3, the corresponding structural elements in the two long toxins superimpose well, both in terms of size and spatial orientation, with those of Chtx. More precisely, the average rms deviation calculated on these elements between the 12 structures of Chtx and either toxin II or variant 3 is 1.20 Å. The different common structural elements are separated by loops with variable size in the three toxins. For instance, the 26 to 29 and 32 to 35 β strands are separated by two residues that form a β turn in both Chtx and variant 3 and by seven residues in toxin II. It appears, thus, that the β sheet, the helix, the

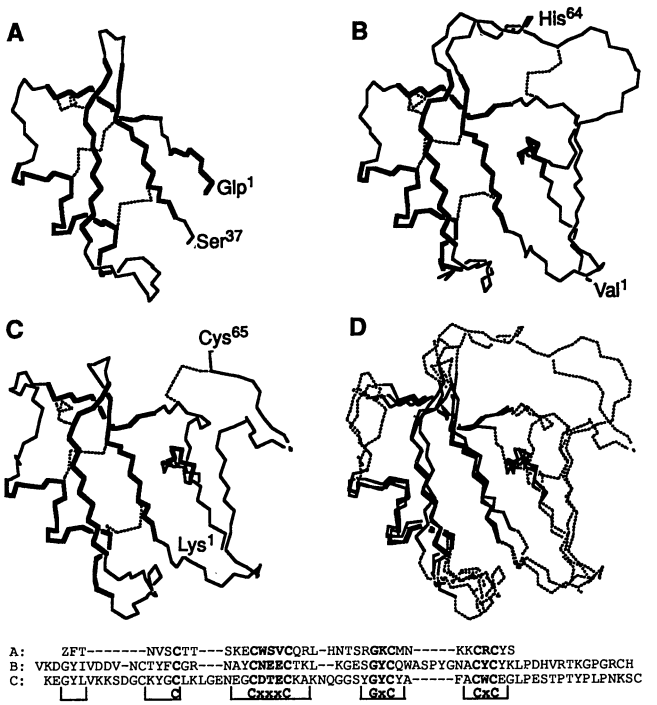

Fig. 3. Comparison of the structures of (**A**) Chtx, (**B**) toxin II of *Androctonus australis Hector*, and (**C**) variant 3 of *Centruroides sculpturatus Ewing*. (A to C) The structures of the three toxins have been redrawn with the same orientation, the disulfides are in dashed lines, and the common structural motif (see text) is indicated by bold lines. (**D**) The three structures have been superimposed. The conserved motif is in plain lines; the disulfides have been omitted for clarity. The three corresponding sequences have been aligned with respect to the conserved structural elements (indicated by the plain boxes below the sequences).

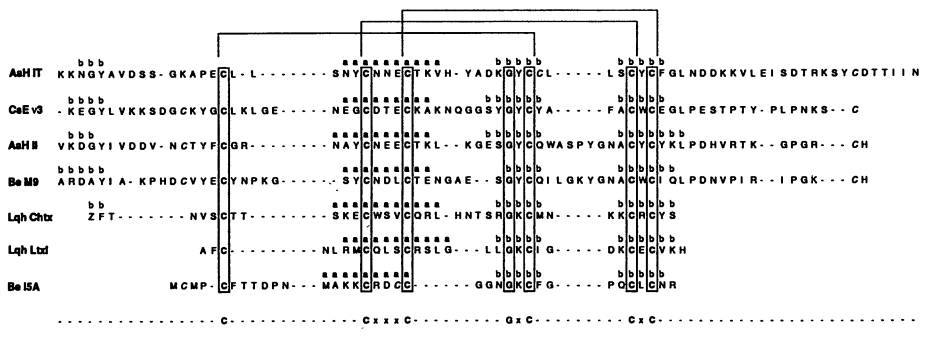

Fig. 4. Comparison of the sequences of scorpion toxins with known secondary structure. The sequences of scorpion toxins have been aligned with respect to the secondary structure elements (a, α helix, and b, β sheet). The consensus sequence (see text) found in these toxins is indicated under the sequences. AaH IT, *Androctonus australis Hector* insectotoxin (*13*); CsE v3, *Centruroides sculpturatus Ewing* variant 3 (*14*); AaH II, *Androctonus australis Hector* toxin II (*15*); Be M9, *Buthus eupeus* toxin M9 (*11*); Lqh Chtx and Ltx I, *Leiurus quinquestriatus hebræus* Chtx and leiurotoxin I (*12*); and Be I5A, *Buthus eupeus* insectotoxin I5A (*10*).

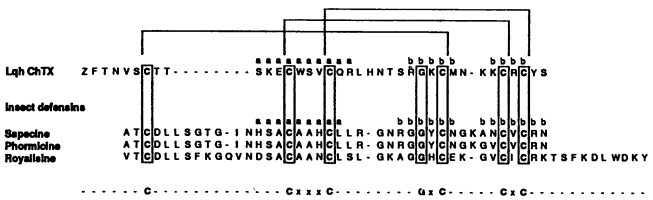

Fig. 5. Comparison of the sequences of Chtx and insect defensins. The sequences of Chtx and insect defensins are aligned with respect to the consensus sequence. This alignment shows that these toxins possess the same secondary structure elements (a, α helix, and b, β sheet) disposed at the same place and linked by the same disulfide bridges. Disulfides bridges have been determined for phormicin (*Phormia terranovae*) (*17*) and sapecin (*Sarcophaya peregrina*) (*19*). Secondary structure elements have been determined for sapecin (*20*). Royalisine is from *Apis mellifera*.

extended fragment, and the three disulfides define a common structural motif to scorpion toxins despite the difference in size, sequence, and biological activity.

Alignment of the sequences of scorpion toxins with the known secondary structure elements (Fig. 4) shows that the structural motif depicted above has a sequential counterpart. The six half-cystines and the glycine present in the motif are the only conserved residues, leading to the following consensus sequence (numbering as in Chtx; aa, amino acid)

$$-\mathrm{Cys}_7-[\ldots]-\mathrm{Cys}_{13}-$$
$$\mathrm{aa}-\mathrm{aa}-\mathrm{aa}-\mathrm{Cys}_{17}-[\ldots]$$
$$-\mathrm{Gly}_{26}-\mathrm{aa}-\mathrm{Cys}_{28}-[\ldots]$$
$$-\mathrm{Cys}_{33}-\mathrm{aa}-\mathrm{Cys}_{35}-[\ldots] \quad (1)$$

The conservation of this sequence appears to be related to well-defined structural requirements as observed in the high-resolution structures of variant 3, toxin II, and Chtx. Thus, the two conserved bridges 13 to 33 and 17 to 35 largely contribute to conserve the relative position of the sheet and the helix. More precisely, the pairing of these two bridges implies that the side chains of the two half-cystines 13 and 17 in the helix point to the same direction as those of the two half-cystines 33 and 35 in the sheet. The proper respective orientation of these side chains is provided by the fact that the two half-cystines in the helix are conservatively separated by three residues (that is, by one helix turn) and the two half-cystines in the β sheet by one residue, respectively. In addition, the helix and the sheet always intersect in the same manner. Interestingly, the limited space at the intersection of the helix and the sheet is occupied by the $H\alpha_2$ proton of Gly^{26}. In this spatial arrangement, no room is left to accommodate any side chain. This observation clarifies the role of the conserved Gly^{26} residue in the consensus sequence of these toxins.

Since the consensus sequence found in the motif seemed reflecting its 3-D organization, we searched in the data bank for proteins from arthropods sharing this sequence. We found it strikingly similar in other small proteins from insects, called insect defensins (*16–18*). These contain ~40 aa residues and three disulfide bonds with pairings identical to those found in Chtx (*17, 19*). Insect defensins are produced in response to body injury, thereby preventing infection by bacteria. We could then readily align the primary structures of three insect defensins with those of scorpion toxins using the above sequential pattern (Fig. 5). Conservation of the pattern could be purely coincidental, but a low-resolution spatial model of one insect defensin reported recently (*20*) revealed that this protein indeed has the same structural motif as found in Chtx. Insect defensins and scorpion toxins could have a common ancestor with a similar 3-D organization.

REFERENCES AND NOTES

1. C. Miller, E. Moczydlowski, R. Latorre, M. Phillipps, *Nature* **313**, 316 (1985).
2. G. Gimenez-Gallego *et al.*, *Proc. Natl. Acad. Sci. U.S.A.* **85**, 3329 (1988).
3. W. Massefski, A. G. Redfield, D. Hare, C. Miller, *Science* **249**, 521 (1990).
4. F. Bontems *et al.*, *Eur. J. Biochem.* **196**, 19 (1991).
5. W. Massefski, A. G. Redfield, D. Hare, C. Miller, *Science* **252**, 631 (1991).
6. H. Takashima *et al.*, *Peptides 1990*, E. Giralt and D. Andreu, Eds. (ESCOM, Leiden, The Netherlands, 1991), pp. 557–559.
7. P. Güntert, W. Braun, K. Wüthrich, *J. Mol. Biol.* **217**, 517 (1991). We acknowledge K. Wüthrich for providing us with a copy of the program.
8. A. T. Brünger, *X-PLOR Manual* (Yale University, New Haven, CT, 1988).
9. M. Simard and D. D. Watt, in *The Biology of Scorpion*, G. A. Polis, Ed. (Stanford Univ. Press, Stanford, CA, 1990), pp. 415–444.
10. A. S. Arseniev, V. I. Kondakov, V. N. Maiorov, V. F. Bystrov, *FEBS Lett.* **165**, 57 (1984).
11. V. S. Pashkov *et al.*, *Biophys. Chem.* **31**, 121 (1988).
12. J. C. Martins, W. Zhang, A. Tartar, M. Lazdunski, F. A. M. Borremans, *FEBS Lett.* **260**, 249 (1990).
13. H. Darbon, C. Weber, W. Braun, *Biochemistry* **30**, 1836 (1991).
14. J. Fontecilla-Camps, R. J. Almassy, F. L. Suddath, C. E. Bugg, *Toxicon* **20**, 1 (1982).
15. J. Fontecilla-Camps, C. Harbersetzer-Rochat, H. Rochat, *Proc. Natl. Acad. Sci. U.S.A.* **85**, 7443 (1988).
16. K. Matsuyama and S. Natori, *J. Biol. Chem.* **263**, 17112 (1988).
17. S. Fujiwara *et al.*, *ibid.* **265**, 11333 (1989).
18. J. Lambert *et al.*, *Proc. Natl. Acad. Sci. U.S.A.* **86**, 262 (1989).
19. T. Kuzuhara, Y. Nakajima, K. Matsuyama, S. Natori, *J. Biochem.* **107**, 514 (1990).
20. H. Hanzawa *et al.*, *FEBS Lett.* **269**, 413 (1990).

21. Abbreviations for the amino acid residues are: A, Ala; C, Cys; D, Asp; E, Glu; F, Phe; G, Gly; H, His; I, Ile; K, Lys; L, Leu; M, Met; N, Asn; P, Pro; Q, Gln; R, Arg; S, Ser; T, Thr; V, Val; W, Trp; and Y, Tyr.

22. We thank E. Quemeneur for performing the sequence research, J. L. Dimarcq for fruitful discussions about insect defensins, and J. Fontecilla-Camp for providing us with the unpublished atomic coordinates of toxin II.

15 July 1991; accepted 24 September 1991